Supporting Information

Laser-induced Graphene Derived from Kraft Lignin for Flexible Supercapacitors

Faisal Mahmood [a, c], Hanwen Zhang [a], Jian Lin [b], Caixia Wan [a, *]

[a] Department of Biomedical, Biological, and Chemical Engineering, University of Missouri, Columbia 65211, USA

[b] Department of Mechanical and Aerospace Engineering, University of Missouri, Columbia 65211, USA

[c] Department of Energy Systems Engineering, University of Agriculture Faisalabad, Faisalabad 38000, Pakistan

[*] Corresponding author: Phone: +1 573 884 7882; Fax: +1 573 884 5650; E-mail: wanca@missouri.edu

Number of Pages: 8

Number of Tables: 1

Number of Figures: 5

1. Characterization

Crystalline size of graphitic carbon in the *a* axis (L_a) was calculated from the intensity ratio of G peak (I_G) to D peak (I_D) from Raman spectra following Equation (1): [1]

$$L_a = (2.4 \times 10^{-10}) \times \lambda_l^4 \times \left(\frac{I_G}{I_D}\right) \qquad (1)$$

where λ_l is the wavelength of the Raman laser (λ_l = 633 nm).

Bending radius (r) of the PDMS-LIG-80 was calculated following Equation (2): [2]

$$r = \frac{h^2 + \frac{d^2}{4}}{2h} \qquad (2)$$

where *h* is the height of the bent device, and *d* is the distance between the two edges of the device. Figure S1 shows the supercapacitor device bent using a Vernier caliber, and the parameters used to calculate its bend radius.

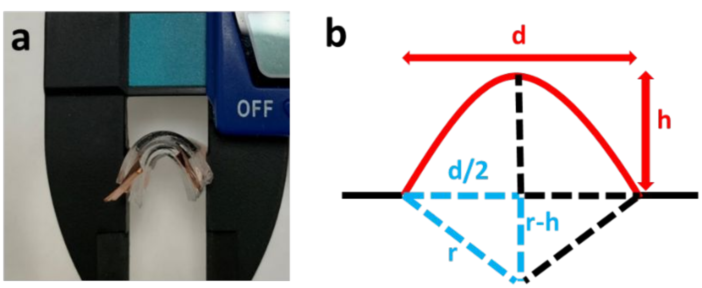

Figure S1. (a) Optical image of LIG-80/PDMS-SC bent using a Vernier caliber. (b) Schematic diagram to display the parameters used to calculate a bend radius of LIG-80/PDMS-SC.

2. Electrochemical analysis

Cyclic voltammetry (CV) and galvanostatic charge-discharge (CD) measurements were conducted on CHI 660D electrochemical workstation (CHI Instruments, USA). The CV tests were carried out at an operating voltage (0 - 1.0 V) with different scan rates ranging from 10 to 500 mV s^{-1}. The CD tests was performed with current densities in a range of 0.01-0.02 mA cm^{-2}.

The specific areal capacitance (C_A, in mF cm^{-2}) based on CV curves was calculated following

Equation (3) below:

$$C_A = \frac{\int_{V_i}^{V_f} I\,dV}{2 \times S \times v \times (V_f - V_i)} \qquad (3)$$

where *S* is the surface area (in cm^2) of an active LIG electrode, with 1 cm^2 for the device configuration in this work; v is the voltage scan rate (in V s^{-1}); V_f and V_i are the potential limits used for the CV analysis (in V); I is the voltammetry current (in A); and $\int_{V_i}^{V_f} I\,dV$ denotes the integrated area of CV curve.

The C_A (in mF cm^{-2}) based on the CD curves was calculated using Equation (4):

$$C_A = \frac{I}{S \times \left(\frac{dV}{dt}\right)} \qquad (4)$$

where I is the discharge current (in A); S is the surface area of the LIG (cm^2), with 1 cm^2 for the device configuration here; and dV/dt is the slope of the galvanostatic discharge curves.

The volumetric capacitance (C_V) (in mF cm^{-3}) was calculated by dividing C_A by the thickness of active material (d, in cm) following Equation (5):

$$C_V = \frac{C_A}{d} \qquad (5)$$

The specific areal and volumetric energy densities (E_A in mWh cm^{-2} and E_v in mWh cm^{-3}, respectively) were calculated following Equations (6) and (7).

$$E_A = \frac{1}{2} \times C_A \times \frac{(\Delta V)^2}{3{,}600} \qquad (6)$$

$$E_V = \frac{1}{2} \times C_V \times \frac{(\Delta V)^2}{3{,}600} \qquad (7)$$

Where $\Delta V = V_{max} - V_{drop}$ is equivalent to the discharge potential range (V_{max} is the voltage of 1 V for H_2SO_4/PVA gel electrolyte); V_{drop} is the voltage drop indicated from the difference of the first two points in the data obtained from the discharge curves.

The specific area and volumetric power densities (P_A, in mW cm^{-2} and P_V, in mW cm^{-3}, respectively) were calculated following Equations (8) and (9).

$$P_A = \frac{E_A}{\Delta t} \times 3{,}600 \qquad (8)$$

$$P_V = \frac{E_V}{\Delta t} \times 3{,}600 \qquad (9)$$

where Δt is the discharge time (in sec).

3. Supplementary results

Table S1. Comparison of graphene-based flexible SCs

Carbon source	**Electrode material**	**Method**	**C_A from CV**	**Scan rate**	**Energy density**	**Power density**	**Ref.**
Kraft lignin	LIG on PDMS	Laser writing	880.25 μF cm^{-2}	10 mV/s	31.3 μWh/cm^{-2}	138 mW cm^{-3}	This work
Graphene	Graphene & gold-deposited PET	Spray coating	840 μF cm^{-2}	10 mV/s	12 mWh cm^{-3}	4.39 mW cm^{-3}	[3]
Polyimide	LIG N-PEDOT	Laser writing	720 μF cm^{-2}	75 μA cm^{-2}	N/A	N/A	[4]
Polyimide	LIG on PDMS	Laser writing	650 μF cm^{-2}	50 mV/s	N/A	N/A	[5]
Graphene oxide (GO)	rGO on PDMS	Photolithography	540 μF cm^{-2}	500 mV/s	0.52 mWh cm^{-2}	417 mW cm^{-2}	[6]
Graphene	Graphene woven fabric	CVD	17 μF cm^{-2}	60 mV/s	N/A	N/A	[7]

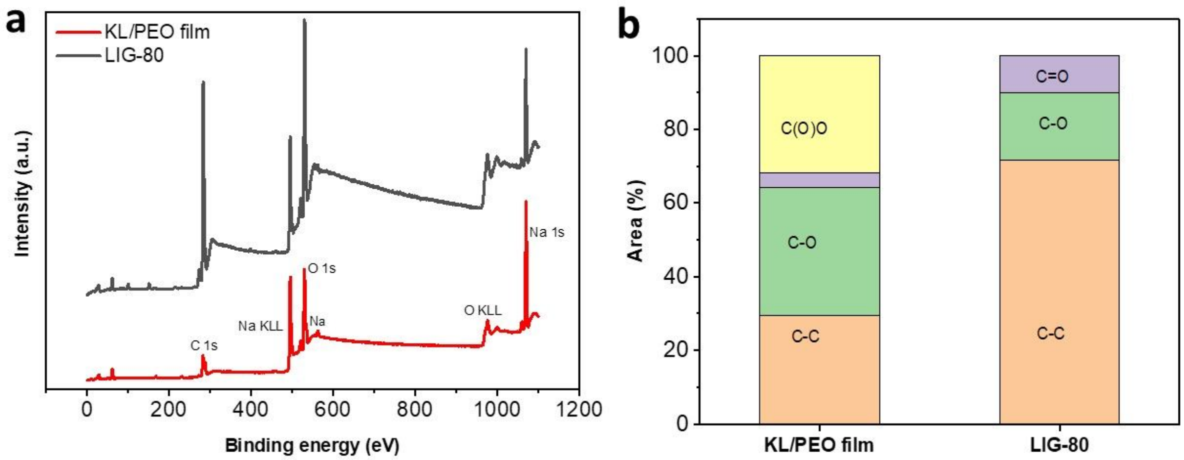

Figure S2. (a) XPS spectra. (b) Functionality revealed by high resolution C1s XPS.

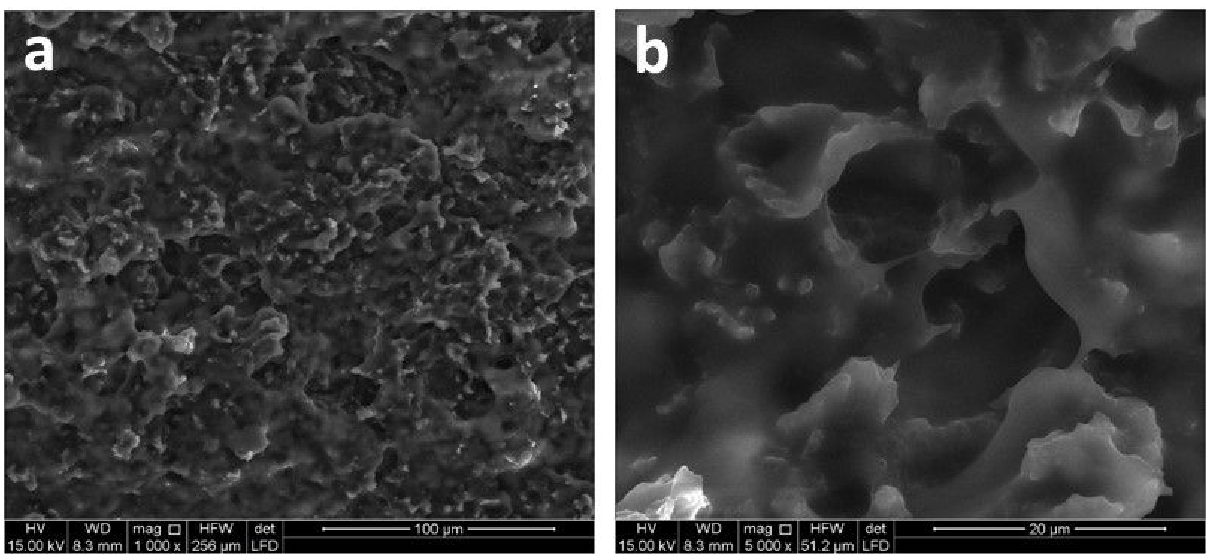

Figure S3. SEM images of the remaining LIG-80 structure after peeling off. (a) Scale bar is 100 μm. (b) Scale bar is 20 μm.

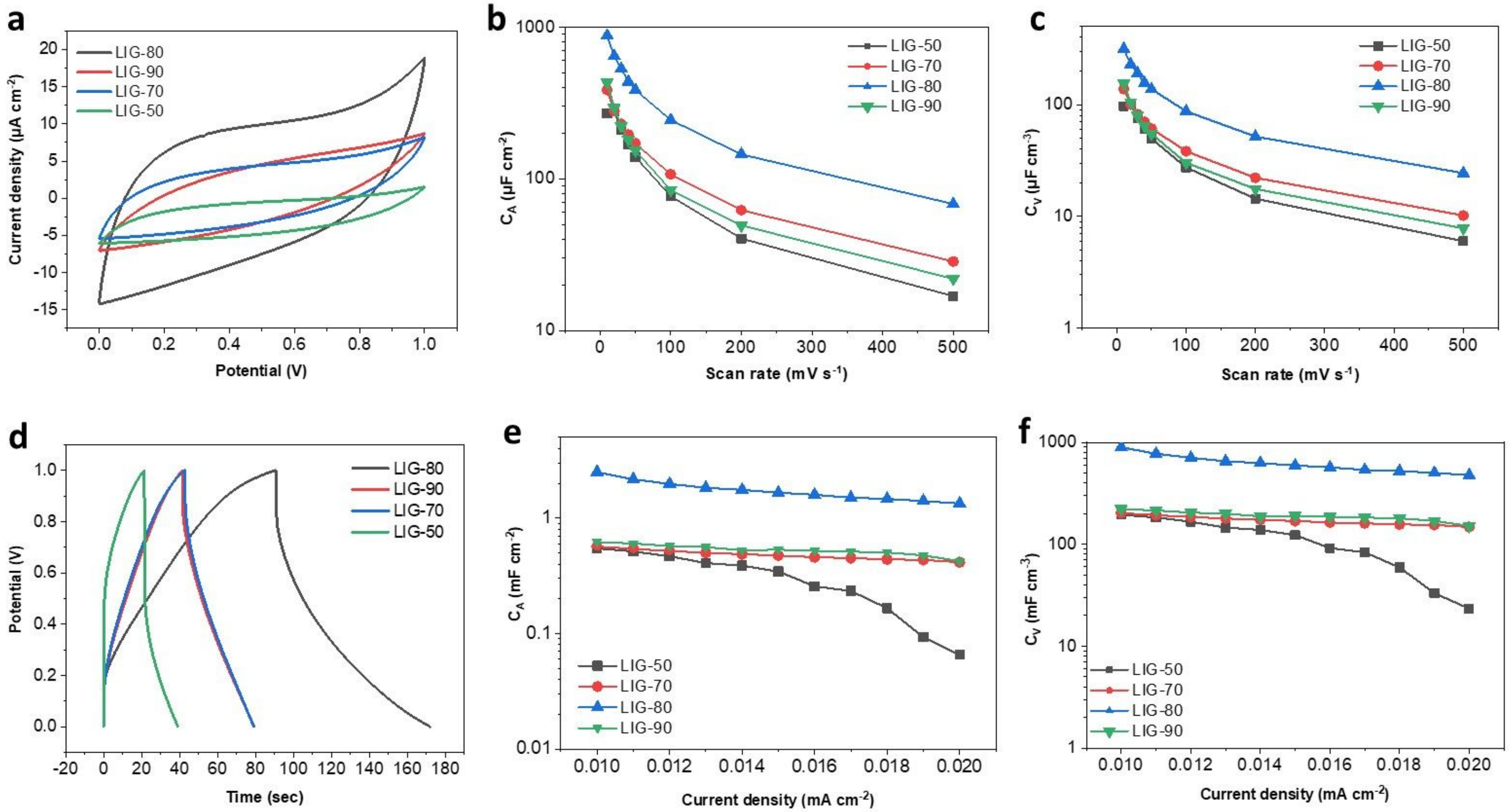

Figure S4. Electrochemical analysis of LIG/PDMS-SC. (a) CV curves obtained at the scan rate of 10 mV s^{-1}. (b, c) Specific areal and volumetric capacitances as a function of scan rate, respectively. (d) CD curves obtained at the current density of 0.01 mA cm^{-2}. (e, f) Specific areal and volumetric capacitances as a function of current density.

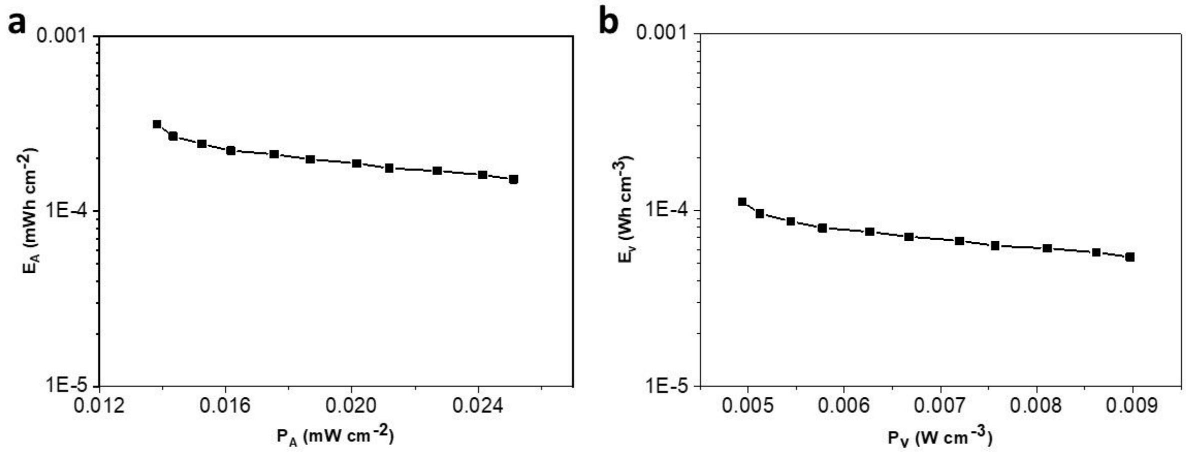

Figure S5. Ragone plots of LIG-80/PDMS-SC. (a) Specific areal energy and current densities. (b) Specific volumetric energy and current densities.

References

(1) Cançado, L.; Takai, K.; Enoki, T.; Endo, M.; Kim, Y.; Mizusaki, H.; Jorio, A.; Coelho, L.; Magalhaes-Paniago, R.; Pimenta, M. J. A. P. L. General equation for the determination of the crystallite size L a of nanographite by Raman spectroscopy. *Appl Phys Lett* **2006,** *88* (16), 163106.

(2) Peng, Z.; Ye, R.; Mann, J. A.; Zakhidov, D.; Li, Y.; Smalley, P. R.; Lin, J.; Tour, J. M. J. A. n. Flexible boron-doped laser-induced graphene microsupercapacitors. *ACS Nano* **2015,** *9* (6), 5868-5875.

(3) Wu, Z.-S.; Liu, Z.; Parvez, K.; Feng, X.; Müllen, K. Ultrathin printable graphene supercapacitors with ac line-filtering performance. *Adv. Mater.* **2015,** *27* (24), 3669-3675.

(4) Song, W.; Zhu, J.; Gan, B.; Zhao, S.; Wang, H.; Li, C.; Wang, J. Flexible, stretchable, and transparent planar microsupercapacitors based on 3D porous laser-induced graphene. *Small* **2018,** *14* (1), 1702249.

(5) Lamberti, A.; Clerici, F.; Fontana, M.; Scaltrito, L. J. A. E. M. A Highly stretchable supercapacitor using laser-induced graphene electrodes onto elastomeric substrate. *Adv. Energy Mater.* **2016,** *6* (10), 1600050.

(6) Qi, D.; Liu, Z.; Liu, Y.; Leow, W. R.; Zhu, B.; Yang, H.; Yu, J.; Wang, W.; Wang, H.; Yin, S.; Chen, X. Suspended wavy graphene microribbons for highly stretchable microsupercapacitors. *Adv. Mater.* **2015,** *27* (37), 5559-5566.

(7) Zang, X.; Zhu, M.; Li, X.; Li, X.; Zhen, Z.; Lao, J.; Wang, K.; Kang, F.; Wei, B.; Zhu, H. Dynamically stretchable supercapacitors based on graphene woven fabric electrodes. *Nano Energy* **2015,** *15*, 83-91.